Heliyon 9 (2023) e23048

Contents lists available at ScienceDirect

Heliyon

journal homepage: www.cell.com/heliyon

Antibacterial effects and microarray-based molecular mechanisms of *trans*-cinnamaldehyde against *Porphyromonas gingivalis*

Ning Gan [a,b,c,1], Yingjing Fang [a,b,c,1], Weimin Weng [a,b,c], Ting Jiao [a,b,c,d,**], Weiqiang Yu [a,b,c,*]

[a] *Department of Prosthodontics, Shanghai Ninth People's Hospital, College of Stomatology, Shanghai Jiao Tong University School of Medicine, Shanghai, 200011, China*
[b] *National Clinical Research Center for Oral Diseases, Shanghai, 200011, China*
[c] *Shanghai Key Laboratory of Stomatology and Shanghai Research Institute of Stomatology, Shanghai, 200011, China*
[d] *Fengcheng Hospital of Fengxian District, Shanghai, 201411, China*

ARTICLE INFO

Keywords:
Trans-cinnamaldehyde
Porphyromonas gingivalis
Antimicrobial activity
Biofilms
Microarray
Gene expression

ABSTRACT

Porphyromonas gingivalis (*P. gingivalis*) is one of the keystone pathogenic bacteria of periodontitis and peri-implantitis. This study aimed to investigate the antibacterial effects and molecular mechanisms of *trans*-cinnamaldehyde (TC), a safe extract from natural plants, on *P. gingivalis*. Minimum inhibitory and minimum bactericidal concentrations (MIC and MBC) of TC were determined, and scanning and transmission electron microscopies were used to assess the morphological changes. The overall biomass was estimated, and the metabolic activity of biofilms was determined at different TC concentrations. A microarray-based bioinformatics analysis was performed to elucidate the underlying molecular mechanisms of TC-inhibited *P. gingivalis*, and significant differences among groups were determined. TC showed an inhibitory effect on the proliferation and survival of planktonic *P. gingivalis*, of which the MIC and MBC were 39.07 μg/mL and 78.13 μg/mL, respectively. TC also significantly suppressed the formation and metabolic activity of *P. gingivalis* biofilm. The results of the significant pathways and gene ontology (GO) analyses revealed that TC treatment inhibited two metabolic pathways, accompanied by the downregulation of relative genes of nitrogen metabolism (*NrfA*, *NrfH*, and *PG_2213*) and starch and sucrose metabolism (*PG_1681*, *PG_1682*, and *PG_1683*). Thus, this study confirmed TC to be a natural antimicrobial agent against *P. gingivalis* and further demonstrated that TC suppressed the microbial activity on *P. gingivalis* through the disruption of physiological metabolism, which might inhibit the growth and the biofilm formation of *P. gingivalis*.

1. Introduction

Periodontitis is one of the most common oral diseases in humans, affecting approximately 10–15 % of the population [1,2]. Severe

* Corresponding author. Department of Prosthodontics, Shanghai Ninth People's Hospital, College of Stomatology, Shanghai Jiao Tong University School of Medicine, Shanghai, 200011, China.
** Corresponding author. Department of Prosthodontics, Shanghai Ninth People's Hospital, College of Stomatology, Shanghai Jiao Tong University School of Medicine, Shanghai, 200011, China.
E-mail addresses: jiao_ting@126.com (T. Jiao), ywqhuai@126.com (W. Yu).
[1] Both authors contributed equally to this work.

https://doi.org/10.1016/j.heliyon.2023.e23048
Received 3 May 2023; Received in revised form 23 October 2023; Accepted 24 November 2023
Available online 29 November 2023

periodontitis can threaten tooth retention, cause the loss of natural teeth, and subsequently adversely impact a person's masticatory function, quality of life, and self-esteem [3]. *Peri-implantitis*, on the other hand, is a common complication after implant repair surgery, which can ultimately lead to implant loosening and even failure if it is not effectively treated and controlled. It is estimated that the mean prevalence of peri-implantitis is 14%–56 % [4]. The number of dental implants used worldwide increases yearly, and the incidence of peri-implantitis cases is expected to rise accordingly [5]. Therefore, concerns about periodontitis and peri-implantitis become increasingly prominent.

The pathogenesis of periodontitis and peri-implantitis is triggered by the dysbiosis of subgingival microbiota, especially linked with Gram-negative anaerobes (including *P. gingivalis*, *Fusobacterium nucleatum*, *Prevotella intermedia*, *Aggregatibacter actinomycetemcomitans*, and so on) [2,6]. Although the existing research is still unable to determine which specific microbiota plays a decisive role in the occurrence and development of these diseases, the current unified view is that *P. gingivalis* is one of the keystone pathogenic bacteria of periodontitis and peri-implantitis [7,8]. *P. gingivalis* together with *Tannerella forsythia* and *Treponema denticola* consist of the red complex organism (the main causative agent in progression of periodontitis). Previous research has found that *P. gingivalis* is also the most frequently detected red complex organism in peri-implantitis sites [6,9,10]. *P. gingivalis* can secrete virulence factors, including FimA protein and gingipain. These virulence factors are closely associated with adhesion characteristics, growth, metabolism, participation in the processing of outer membrane proteins, and the formation of *P. gingivalis* biofilms [11]. The virulence proteins derived from *P. gingivalis* can indirectly stimulate host defence cells to produce many inflammatory factors, further degrade collagens, and destroy tissues [4]. Moreover, *P. gingivalis* is one of the most commonly used pathogens to induce experimental periodontitis and peri-implantitis in animal models [12–14]. It has been reported to enhance the survival of other oral pathogens, change the originally balanced flora structure in the periodontal pocket, cause an imbalance of flora and periodontal microenvironment, and thus aggravate the damage to periodontal tissues [15]. *P. gingivalis*, even in low abundance, may lead to inflammatory disease occurrence around natural teeth and dental implants [16]. Therefore, adjunctive use of antibiotics against *P. gingivalis* are thought to be effective in preventing and treating periodontitis and peri-implantitis at an early stage.

Currently, natural herbs and medicines have become important options owing to their unique properties, which may avoid the toxicological effects of synthetic pharmaceutical products and the side effects of antibiotics without increasing the antibacterial resistance of bacteria [17]. Plant essential oils are regarded as potential antibiotic substances because of their main components, phenolic acids, among which eugenol, cinnamaldehyde, and citral have the most potent antibacterial effect [18,19]. *Trans*-cinnamaldehyde (TC; C_9H_8O) is a bioactive compound obtained from the bark of *Cinnamomum cassia* that has been recognised as a safe and non-toxic food ingredient, and is approved by the US Food and Drug Administration (21CFR182.60) [17,20]. In addition, TC has various biological activities, including antioxidant [21,22], anti-inflammatory [20,23] and anti-cancer effects [24,25], as well as enhancing diabetes treatment [26,27]. TC is a widely acknowledged antimicrobial, with demonstrated efficacy against both Gram-negative and Gram-positive bacteria [28]. It also has a good inhibitory effect against some oral pathogenic bacteria, including *Streptococcus mutans* [29,30], *P. gingivalis* [17], *Enterococcus faecalis* [31], *Escherichia coli*, and *Staphylococcus aureus* [32,33]. The oral administration of cinnamaldehyde was reported to inhibit the progress of murine periodontitis with significant suppression of microbiota dysbiosis [20]. A previous study found that cinnamaldehyde showed inhibitory action against *P. gingivalis* via damage to the cell membrane structure [17]. However, the inhibitory effect of TC on the biological pathways of *P. gingivalis* and its mechanism of action has rarely been studied. Therefore, this study aimed to investigate the antibacterial activity of TC on *P. gingivalis* and to detect its possible antibacterial mechanism through microarray-based bioinformatics analysis, attempting to provide further insight into the potential of TC to be used in adjunctive treatment of periodontitis and peri-implantitis.

2. Materials and methods

2.1. Preparation of TC stock solution

TC (≥99 % purity) was purchased from Sigma–Aldrich (St. Louis, MO, USA), and was dissolved in a brain-heart infusion (BHI, Oxoid Ltd., England) to a concentration of 5 mg/mL as the stock solution. Afterwards, the TC stock solution was taken in serial two-fold dilutions to obtain different concentrations ranging from 4.88 to 312.50 μg/mL for the following experiments.

2.2. Microbial cultivation

P. gingivalis strain (ATCC 33277) was provided by the Laboratory of Oral Microbiota and Systemic Diseases, Shanghai Ninth People's Hospital, College of Stomatology, Shanghai Jiao Tong University School of Medicine, and grown under previously reported conditions [34]. Planktonic *P. gingivalis* was cultivated in BHI broth supplemented with 5 mg/L hemin and 1 mg/L menadione for 24 h and then diluted to obtain a bacterial suspension of 10^7 colony-forming units per milliliter (CFU/mL) for the following experiments.

2.3. Determining MIC and MBC

A 500 μL *P. gingivalis* suspension (10^7 CFU/mL) was cultivated with 500 μL of different TC solutions in each test tube, serving as the experiment groups. A culture medium without bacteria was used as the positive control, and an untreated *P. gingivalis* suspension was used as the negative control. After incubation for 48 h at 37 °C under anaerobic conditions, a 200 μL sample of each group was transferred to a 96-well tissue culture plate to measure the optical density (OD) values using a microplate reader (Epoch 2, Bio-Tek Instruments, Winooski, VT, USA). The 100 μL suspension of each group was plated onto blood agar plates. The experiment was

conducted in triplicate for each group. After 5 days of incubation, the plates were photographed to record the growth of the bacterial colonies.

2.4. Membrane permeability assay

A 500 μL *P. gingivalis* suspension (10^7 CFU/mL) was added to a 1.5 mL centrifuge tube and then incubated with 500 μL TC solution at 1/4 × MIC, 1/2 × MIC, 1 × MIC, and 2 × MIC, individually, under a 37 °C anaerobic environment for 4 h. *P. gingivalis* suspension and culture medium were mixed in equal volumes (500 μL each), serving as the control. Propidium iodide (PI; Molecular Probes, Eugene, OR, USA) was incubated with suspension in each group for 15 min in the dark, and the stained bacteria were observed using a confocal laser scanning microscope (CLSM; Zeiss LSM 880, Germany). The excitation/emission wavelength was 543 nm for PI.

2.5. Morphological changes in P. gingivalis

After *P. gingivalis* suspensions (10^7 CFU/mL) were co-cultured with TC solution at 1/4 × MIC, 1/2 × MIC, and 1 × MIC for 4 h individually, the bacteria were collected by centrifugation at 3000 rpm for 5 min at 4 °C. Subsequently, the pellets were separately fixed with 2.5 % v/v glutaraldehyde at 4 °C for 12 h. For the observation of the morphological changes using scanning electron microscopy (SEM), the samples were dehydrated in a series of ethanol solutions (30 %, 50 %, 70 %, 80 %, 90 %, and 95 % once for 15 min each, followed by 100 % ethanol twice for 20 min each), and then dried at the CO_2 critical point. Finally, the samples were sputter-coated with gold and viewed using SEM (SU3050, Hitachi, Japan). Moreover, for transmission electron microscopy (TEM) observation, the samples were washed with phosphate buffered solution (PBS) and then fixed in 1 % (w/v) osmium tetroxide (OsO_4) for 2 h. After sequential dehydration in a series of ethanol solutions followed by acetone (80 %, 90 %, and twice in 100 % for 15 min each), the samples were embedded and sliced at approximately 70 nm using an ultrathin microtome (Leica EM UC7, Germany). Subsequently, these sections were stained with lead citrate solution and 50 % ethanol-saturated solution of uranium dioxide acetate for 10 min. After drying, the samples were scanned using TEM (HT7800, Hitachi, Japan) at 80 kV.

2.6. Overall biomass of biofilms

A 500 μL *P. gingivalis* suspension (10^7 CFU/mL) was seeded with 500 μL TC at 1/4 × MIC, 1/2 × MIC, and 1 × MIC in each well of a 24-well tissue culture plate. After co-culturing under a 37 °C anaerobic environment for 48 h, supernatants were discarded, and 250 μL crystal violet solution (0.1 % v/v, Sangon Biotech, China) was added to each well for 15-min incubation at room temperature. After washing thrice with PBS, 250 μL of 95 % ethanol (v/v, Tong Cheng Chemical Agent Co., Ltd., China) was added to each well for 15 min. Subsequently, the solutions were transferred to a 96-well plate, and the overall biomass was estimated using a microplate reader at 595 nm. The experiment was conducted in triplicate for each group.

2.7. Metabolic activity of biofilms

After co-culturing 500 μL *P. gingivalis* suspensions (10^7 CFU/mL) with 500 μL TC at 1/4 × MIC, 1/2 × MIC, and 1 × MIC for 48 h individually, the culture supernatants were removed, and 250 μL MTT (0.5 mg/mL, Sangon Biotech, China) was added to each well for 4-h incubation at 37 °C in the dark. Subsequently, each well was washed with PBS thrice, and 250 μL dimethyl sulfoxide (DMSO, Tong Cheng Chemical Agent Co., Ltd., China) was added to each well to dissolve the formazan crystals, and was shaken for 15 min. Finally, the DMSO supernatants were transferred to a 96-well plate, and the OD values were recorded at a wavelength of 490 nm. The experiment was conducted in triplicate for each group.

2.8. Live/dead fluorescence staining of biofilms

500 μL *P. gingivalis* suspensions were inoculated into confocal dishes and cultured with 500 μL TC at 1/4 × MIC, 1/2 × MIC, and 1 × MIC, individually. After 48 h, the LIVE/DEAD BacLight Bacterial Viability Kit (Molecular Probes, Eugene, OR, USA) was used to stain live and dead bacteria in biofilms formed by different groups. According to the manufacturer's instructions, a mixed solution of PI and SYTO 9 (1.5 μL each diluted in 1 mL of ddH_2O) was incubated with bacteria from different groups for 15 min in the dark, and subsequently, the biofilm structure was observed using CLSM. The excitation/emission wavelengths were 543 and 488 nm for PI and SYTO 9, respectively.

2.9. Transcriptome sequencing analysis

The experiment samples were divided into two groups. *P. gingivalis* grown in a normal culture medium was used as the control group, whereas those cultured with TC at 1/2 × MIC were the test group. After 48 h of incubation, *P. gingivalis* cells from the two groups were harvested and processed for transcriptome sequencing analysis, which was conducted in triplicate for each group. Total RNA was extracted using TRIzol reagent (Sigma, USA) from *P. gingivalis* cells according to the manufacturer's protocol.The quality and concentration of extracted RNA were analysed using a Nanodrop 1000 (Thermo Scientific Inc., Wilmington, DE, USA), and the integrity was verified by agarose gel electrophoresis. After the quality inspection, an RNA library was constructed using standard procedures. The samples were operated in Novaseq 6000 (Illumina, USA). The original data were converted into FASTQ format. Based on the

experiment design, DESeq2 software was used to screen differentially expressed genes between the test and control groups, with inclusion criteria ($|\log2FC| \geq 1$ and P value ≤ 0.05).

2.10. GO and kyoto encyclopedia of genes and genomes (KEGG) analysis

The functions of the differentially expressed genes were analysed using the GO project (http://www.geneontology.org/). The analysis involved three GO categories, including biological processes, cellular component, and molecular function. The significant pathways of the identified genes were performed using the KEGG project (https://www.genome.jp/kegg/). Fisher's exact test was used to obtain a significantly-rich P-value, which was then corrected using the Benjamini and Hochberg multiple tests to obtain false discovery rate (FDR). The functions and pathways were significantly enriched according to the P value ($P \leq 0.05$) [35,36].

2.11. Quantitative reverse transcription polymerase chain reaction (RT-qPCR)

After treatment with TC solutions of 1/2 × MIC for 48 h under 37 °C anaerobic environment, the bacterial suspensions were harvested and added to lysozyme and proteinase K (Sangon Biotech, China). After placement in the water bath and centrifugation, the pellets were resuspended in TRIzol reagent and treated with chloroform, isopropanol, and 75 % ethanol (DEPC water) to extract total RNA. Relevant cDNA was obtained using a reverse transcription kit (Yeason Biotechnology Co., Ltd., Shanghai, China) and then further amplified with an SYBR Green Master Mix kit (Yeason), according to the manufacturer's instructions. *16S rRNA* gene was used as an internal control for data normalisation. Table 1 shows the primers (Sangon Biotech, Shanghai, China) used. RT-qPCR was conducted using LightCycler 480 (Roche Diagnostics, Basel, Switzerland). The PCR conditions included initial denaturation at 98 °C for 5 min, followed by a 40-cycle amplification consisting of denaturation at 98 °C for 15 s, annealing at 60 °C for 15 s, and extension at 72 °C for 30 s. The cycle threshold (CT) values were read for statistical analysis. The relative changes in gene expression in TC-treated *P. gingivalis* compared with those in the control group were calculated using the $2^{-\Delta\Delta CT}$ method.

2.12. Statistical analysis

A minimum sample size of n = 3 was used for all statistical analyses, and data are presented as mean ± standard deviation. Significant differences among groups were determined using an unpaired two-tailed Student's t-test or one-way analysis of variance (ANOVA) and Dunnett's test. Statistical analyses were performed using the GraphPad PRISM software (v8.2.1; GraphPad, La Jolla, CA, USA). Statistical significance was set as $P \leq 0.05$.

3. Results

3.1. Antibacterial effects of TC on planktonic P. gingivalis

As shown in Fig. 1A, OD values revealed that increasing concentrations of TC had a significant inhibitory effect on the growth of *P. gingivalis* in broth. The MIC was equivalent to the concentration of the tube without visible growth [37]. TC at a final concentration of 39.07 μg/mL almost completely suppressed the growth of planktonic bacteria, which was regarded as its MIC against *P. gingivalis*. The MBC was determined as the minimum concentration in the area of the agar plate without any bacteria [38]. As shown in Fig. 1B, a TC of 78.13 μg/mL and above inhibited the growth of *P. gingivalis* on the plate after 5-day cultivation and was regarded as its MBC.

3.2. Effect of TC on membrane permeabilization of P. gingivalis

PI, a nucleic acid red fluorescent dye, cannot penetrate the cell membrane of living cells but can only stain dead cells whose cell membrane integrity has been damaged. Therefore, the membrane permeabilization of *P. gingivalis* was evaluated using a PI uptake assay [17]. As shown in Fig. 2A–E, more bacteria were stained red when incubated with TC than those in unexposed control cells. As shown in Fig. 2F, the number of stained bacteria in regions of interest (ROIs) were 60.00 ± 7.81, 390.33 ± 77.84, 498.00 ± 36.06, 1027.00 ± 30.00, and 3667.33 ± 309.65 in the control group, for 1/4 × MIC, 1/2 × MIC, 1 × MIC, and 2 × MIC, respectively, indicating that TC enhanced the membrane permeabilization of *P. gingivalis* with increasing concentrations.

Table 1
Primer sequences used in RT-qPCR.

Genes	Forward	Reverse
NrfH	CGGCAAGTCAGGCGGTAATCTATG	TCTCTGTGGCAGTCCCAGCATG
NrfA	GCCATACATAAGCGAAGGAGGAGTG	ACGGTGACAGGTCTGACAGGTG
PG_2213	CTGCCACTGCAACGAAATTACACG	CGCCTACTTCATCCACGGTCTTC
PG_1681	GTGGCAAACAAGAAGAACGGGAAC	AACGCAGATAGGCTTCGGTGTATTG
PG_1682	GCCGACCGCTTCCACTTCAC	CGGATACGGATGGCATCACATAGAC
PG_1683	TCACGGAAGGAGCCAAACACATAC	CATCGCTCAGCCTCGGATTGC
16S rRNA	TGTAGATGACTGATGGTGAAA	ACTGTTAGCAACTACCGATGT

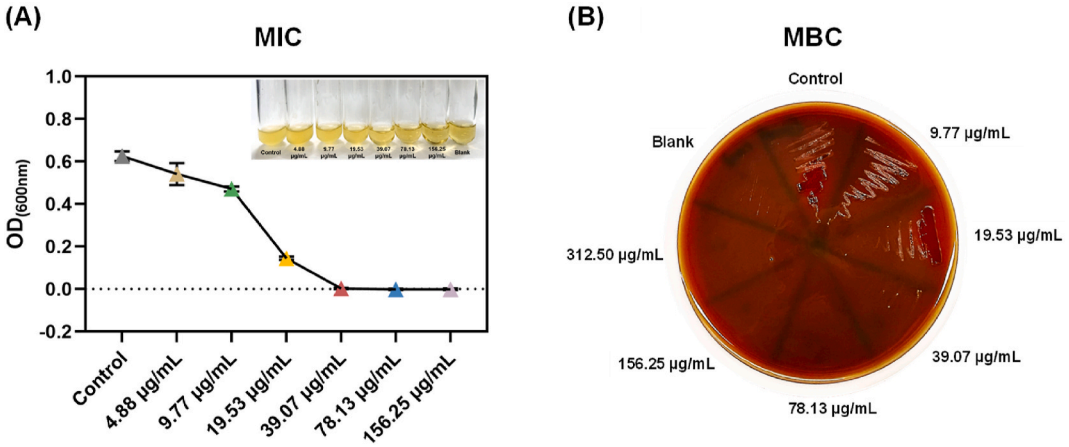

Fig. 1. Antibacterial effects of *trans*-cinnamaldehyde against planktonic *P. gingivalis*. (A) MIC; (B) MBC.

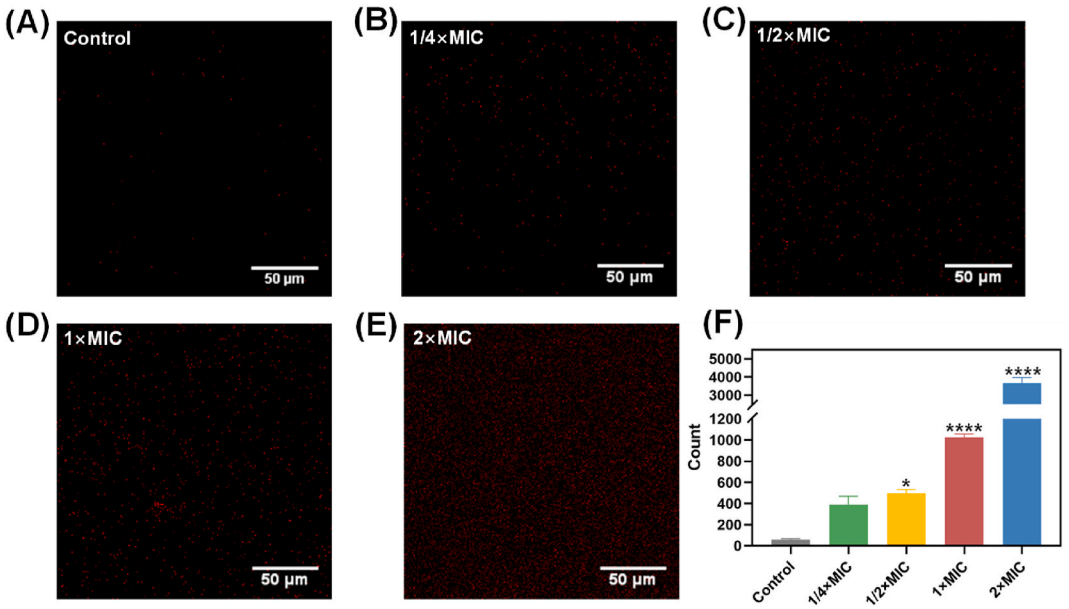

Fig. 2. Membrane permeabilization of *P. gingivalis*. (A) Control; (B) 1/4 × MIC; (C) 1/2 × MIC; (D) 1 × MIC; (E) 2 × MIC; (F) Semi-quantitative evaluation of membrane-permeabilized *P. gingivalis* in each group. Values are presented as mean ± SD with n = 3. Statistical significance was assessed using one-way ANOVA and Dunnett's test. *$P < 0.05$ and ****$P < 0.0001$.

3.3. Morphological changes in P. gingivalis

SEM was used to detect morphological changes in *P. gingivalis* co-cultured with TC, and showed that the untreated *P. gingivalis* cells had normal and complete morphologies (Fig. 3A and E, blue arrows pointing to normal cells) with more intercellular substances. Deformed *P. gingivalis* was observed after treatment with TC (Fig. 3B–D and F–H, red arrows indicate abnormal cells); for instance, some bacteria were shrivelled and some were discontinuous.

TEM was performed to examine the morphological changes and intracellular modifications of treated *P. gingivalis*. Fig. 3I and M (blue arrows) show a clear peptidoglycan layer and cytoplasmic membrane of normal *P. gingivalis*, while obvious morphological changes were observed in the cells treated with TC. Fig. 3J and N (indicated by the red arrows) illustrate that the cell walls are damaged with a fuzzy boundary, and Fig. 3O shows cytoplasmic membranes separated from the cell wall. Moreover, compromised cell walls and the outflow of cytoplasm were detected, as shown in Fig. 3K and L; meanwhile, Fig. 3P demonstrates that the cell hollow resulted from the outflow of cytoplasm, indicating the death of bacterial cells.

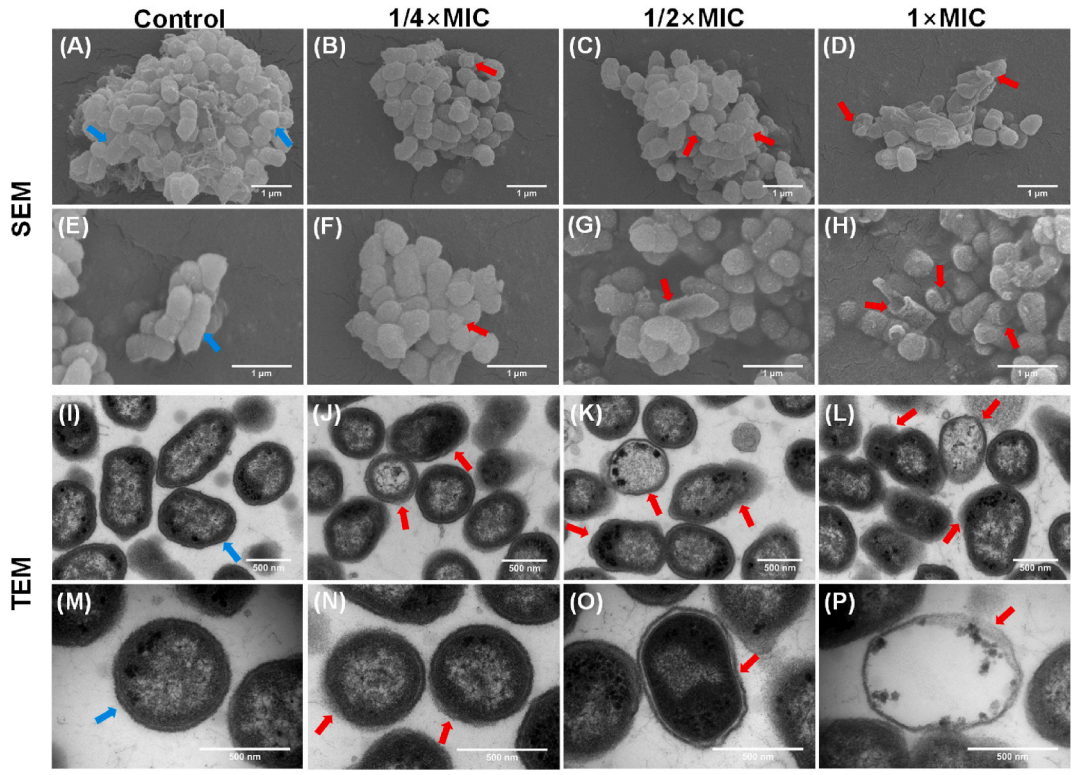

Fig. 3. Representative SEM and TEM images of untreated *P. gingivalis* and treated *P. gingivalis* with TC. (A and E) SEM micrographs of untreated *P. gingivalis*. SEM micrographs of treated *P. gingivalis* with TC at 1/4 × MIC (B and F), 1/2 × MIC (C and G) and 1 × MIC (D and H) for 4 h. (I and M) TEM micrographs of untreated *P. gingivalis*. TEM micrographs of treated *P. gingivalis* with TC at 1/4 × MIC (J and N), 1/2 × MIC (K and O) and 1 × MIC (L and P) for 4 h. Blue and red arrows point to normal and abnormal bacteria, respectively. For the SEM images, scale bars represents 1 μm. For the TEM images, scale bars represents 500 nm.

3.4. Effect of TC on *P. gingivalis* biofilm

As shown in Fig. 4A, the biomasses of biofilms formed after treatment with TC at 1/4 × MIC, 1/2 × MIC, and 1 × MIC were 91.40 ± 1.57 %, 85.08 ± 2.28 %, and 35.31 ± 1.87 %, respectively, compared with the control. Fig. 4B shows that the relative bacterial activities of biofilms after treatment with TC at 1/4 × MIC, 1/2 × MIC, and 1 × MIC were 90.23 ± 1.41 %, 41.80 ± 1.27 %, and 5.64 ± 0.34 %, respectively, compared to the control group. These results revealed that TC inhibited the formation of *P. gingivalis* biofilms and the metabolic activity of cells in biofilms.

Furthermore, live/dead double staining was performed to investigate the changes in cell viability in *P. gingivalis* biofilms after treatment with TC, which further supported the results of the MTT assay. As shown in Fig. 4C, fewer bacteria were stained green, while a larger number of bacteria were stained red in the TC-treated group than in the control group, indicating that TC at 1/4 × MIC, 1/2 × MIC, and 1 × MIC inactivated *P. gingivalis* cells and reduced biofilm formation.

3.5. Transcriptome sequencing data analysis

According to differential cut-off criteria ($|\log2FC| \geq 1$ and P value ≤ 0.05), heat map analysis showed that TC at 1/2 × MIC cultivation induced a significant alteration in gene expression in *P. gingivalis* compared with normal cultivation (Fig. 5A). Overall, 86 differentially expressed genes in *P. gingivalis* cells were identified when comparing the test group with the control group (Table S1). Notably, 40 genes were upregulated and 46 were downregulated following exposure to TC at 1/2 × MIC for 48 h (Fig. 5B).

Fig. 6A and B shows the main GO categories. The main GO categories for downregulated genes were related to biological processes such as oxidation-reduction processes, generation of precursor metabolites and energy, and nitrate metabolic processes (Fig. 6A). The downregulated genes of cellular components were related to chloroplasts and plastids, whereas those of molecular functions were related to haeme binding, nitrite reductase activity, and tetrapyrrole binding. The biological processes for upregulated genes were related to butyrate, short-chain fatty acid, and fatty acid metabolic processes (Fig. 6B). The upregulated genes of cellular components were correlated with ribosome and ribonucleoprotein complexes, while those of molecular functions were related to the structural constituents of ribosomes and structural molecule activity. Tables S2 and S3 show differentially expressed genes.

According to KEGG pathway analysis, two downregulated biological pathways were enriched and three upregulated biological

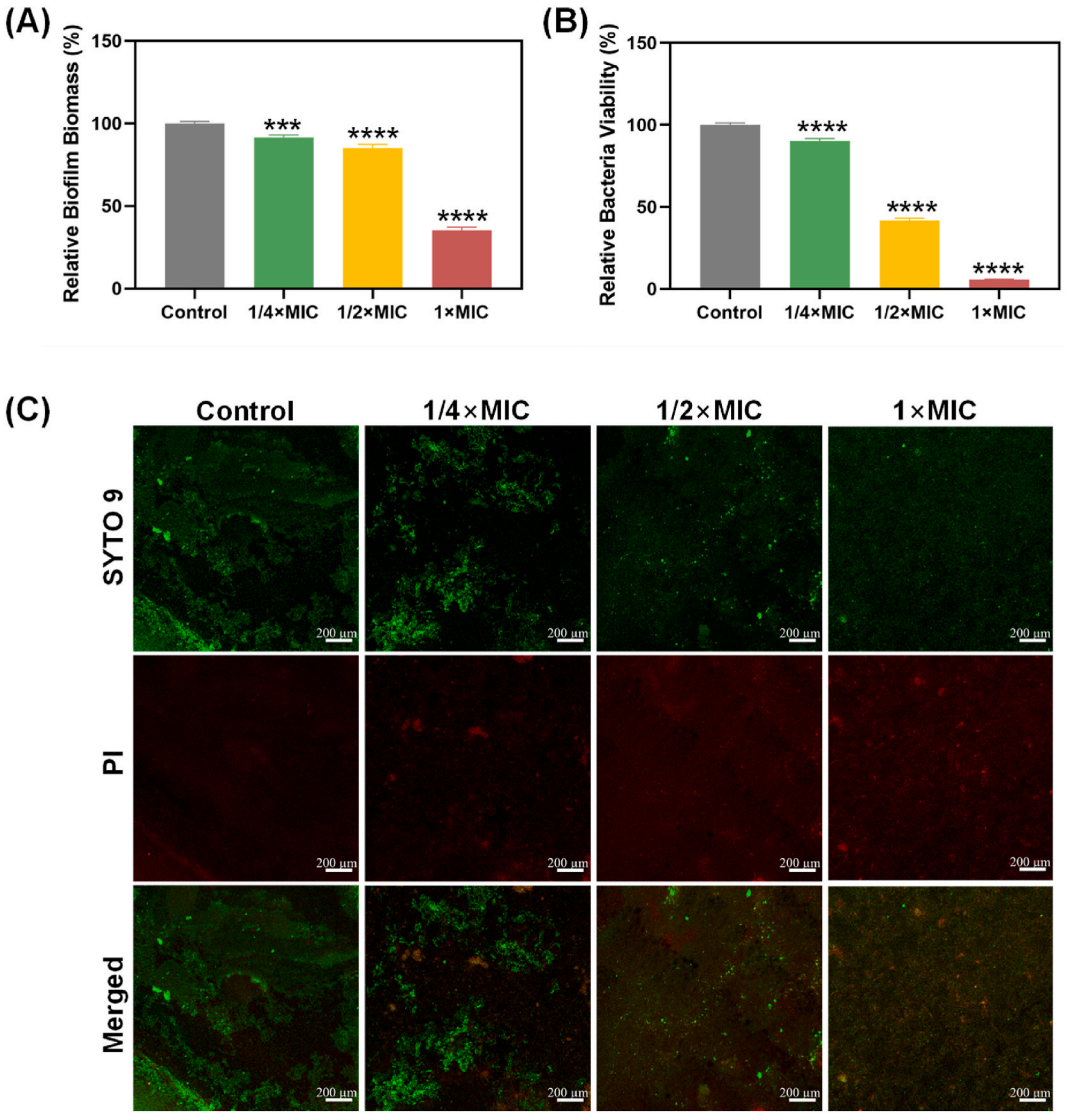

Fig. 4. Antibiofilm effects of *trans*-cinnamaldehyde against *P. gingivalis*. (A) Relative biofilm biomass in each group at 48 h. (B) Relative bacterial activity. Values are presented as mean ± SD with n = 3. Statistical significance was assessed using one-way ANOVA and Dunnett's test. ***$P < 0.001$ and ****$P < 0.0001$. (C) Fluorescent images of untreated *P. gingivalis* biofilms and treated biofilms with TC. Bacteria in biofilms were stained with SYTO 9 (green: live) and PI (red: dead). Scale bars, 200 μm.

pathways were enriched in *P. gingivalis* grown with TC at 1/2 × MIC (Fig. 6C and D). The downregulated biological pathways included nitrogen metabolism, and starch and sucrose metabolism (Fig. 6C). The upregulated biological pathways included ribosome, lipopolysaccharide biosynthesis, and nicotinate and nicotinamide metabolism (Fig. 6D). Table S4 shows differentially expressed genes.

3.6. Validation by RT-qPCR

Six genes that showed significant differential expression in RNA-seq were validated using RT-qPCR. As shown in Fig. 7, the expression levels of selected genes related to nitrogen metabolism (*NrfA*, *NrfH*, and *PG_2213*) and starch and sucrose metabolism (*PG_1681*, *PG_1682*, and *PG_1683*) were significantly downregulated after treatment with TC at 1/2 × MIC compared with the control group.

4. Discussion

Antimicrobial potential is often assessed according to MIC values. It has been reported that the antibacterial effect of natural products is classified based on the following MIC: <500 μg/mL (strong), 600–1500 μg/mL (moderate), and >1600 μg/mL (weak) [39].

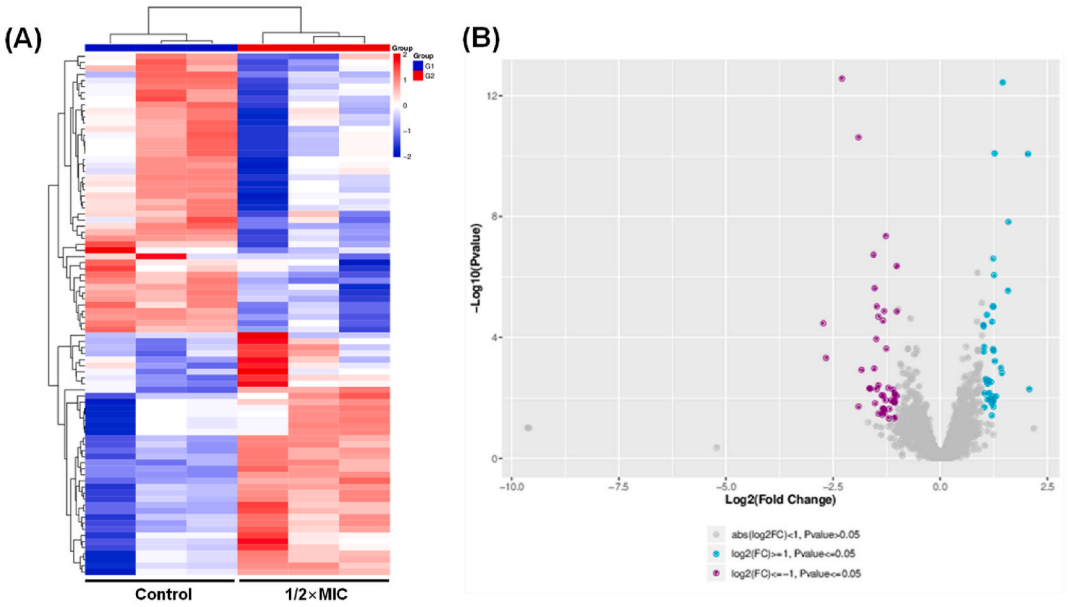

Fig. 5. Differential expression gene screening. (A) Heat map of significantly different genes of *P. gingivalis* cells grown with normal culture medium (G1) vs. TC at 1/2 × MIC (G2). (B) Bubble plots of gene expression when comparing *P. gingivalis* cells grown with TC at 1/2 × MIC vs. normal culture medium. The blue bubbles represent upregulated genes, purple bubbles represent downregulated genes, and grey bubbles represent unregulated genes.

In this study, the MIC of TC on *P. gingivalis* was 39.07 μg/mL, which was considered a strong inhibitor of *P. gingivalis*. The MBC of TC against *P. gingivalis* was determined to be 78.13 μg/mL, which was twice the MIC, indicating the bactericidal potential of TC. In previous research, Wang et al. confirmed that cinnamaldehyde was the main constituent responsible for the antibacterial property of *Cinnamomum zeylanicum* and the MIC of cinnamaldehyde against *P. gingivalis* was 2.5 μM [17]. Saquib et al. investigated the antimicrobial effect of the ethanolic extract of *Cinnamomum zeylanicum* on *P. gingivalis* and found that the MIC and MBC were 3.12 ± 0.65 mg/mL and 12.5 ± 1.35 mg/mL, respectively [40]. The relatively wide range of MICs may be due to differences in the purity or extraction methods of cinnamaldehyde.

In the membrane permeability assay, more red fluorescence was detected after treatment with TC at 1 × MIC and 2 × MIC. This finding revealed that TC increased the membrane permeabilization of *P. gingivalis* cells and killed the bacteria. SEM and TEM analyses further confirmed the same result for PI intake detection. After co-culturing with TC, some *P. gingivalis* cells emerged with abnormal shape, incomplete membrane, separated cell membrane from the cell wall, outflow of cytoplasm, and finally collapsed. *P. gingivalis* cells, therefore, had difficulty proliferating and surviving in the presence of TC. When bacteria adhere to a surface, biofilm formation begins almost immediately [41]. Meanwhile, preventing biofilm formation is the most effective way to inhibit the onset and development of periodontitis and peri-implantitis [42]. In this study, less overall biomass of biofilms was formed after exposure to TC, demonstrating the anti-biofilm potential of this natural extract. Moreover, the cell viability assessment and live/dead fluorescence staining together reached a similar conclusion that fewer live bacterial cells existed in treated biofilms. These results revealed that TC could inhibit the activity and growth of *P. gingivalis*; thus, it was not easy for these bacteria to adhere and form biofilms.

Furthermore, we performed a microarray-based bioinformatics analysis to elucidate the underlying molecular mechanisms of TC-inhibited *P. gingivalis* and found that 40 and 46 genes were upregulated and downregulated, respectively, in *P. gingivalis* cultured with TC at 1/2 × MIC. Furthermore, some gene functions and signaling pathways may control *P. gingivalis* behavior when exposed to TC. The prominent biological processes of the upregulated genes compared to the test group were metabolic processes, especially the butyrate metabolic process. Previous researches have been conducted on the butyrate metabolic process of intestinal bacteria [43,44]. Butyrate exhibits various pharmacological activities, including anti-inflammatory, antioxidant, and metabolic pathway regulatory activities [45]. Our results not only partially explained the reason for TC in the treatment of aggressive periodontitis, considering the importance of the "Gum–Gut" Axis [46], but also provided a new idea on the mechanism of TC for the treatment of other inflammatory diseases [47,48]. The upregulated genes that correlated with cellular components and molecular functions were primarily concentrated in the ribosome, which is the cell's protein-synthesising factory. Although the ribosome has been reported to be an important antibiotic target in bacterial cells [49], TC might activate different mechanisms in this study. The downregulated genes related to cellular components included chloroplasts, in which photosynthetic bacteria could use light under anaerobic conditions to convert carbon dioxide into organic carbon [50]. Natural TC might show antimicrobial activity with distinct target sites, which requires verification in future studies. The downregulated genes in biological processes were mainly found in the oxidation-reduction process, precursor metabolites and energy generation, and nitrate metabolic processes. Downregulated oxidation-reduction processes might destroy the balance between the production of reactive oxygen species and antioxidant defences, which would induce oxidative stress

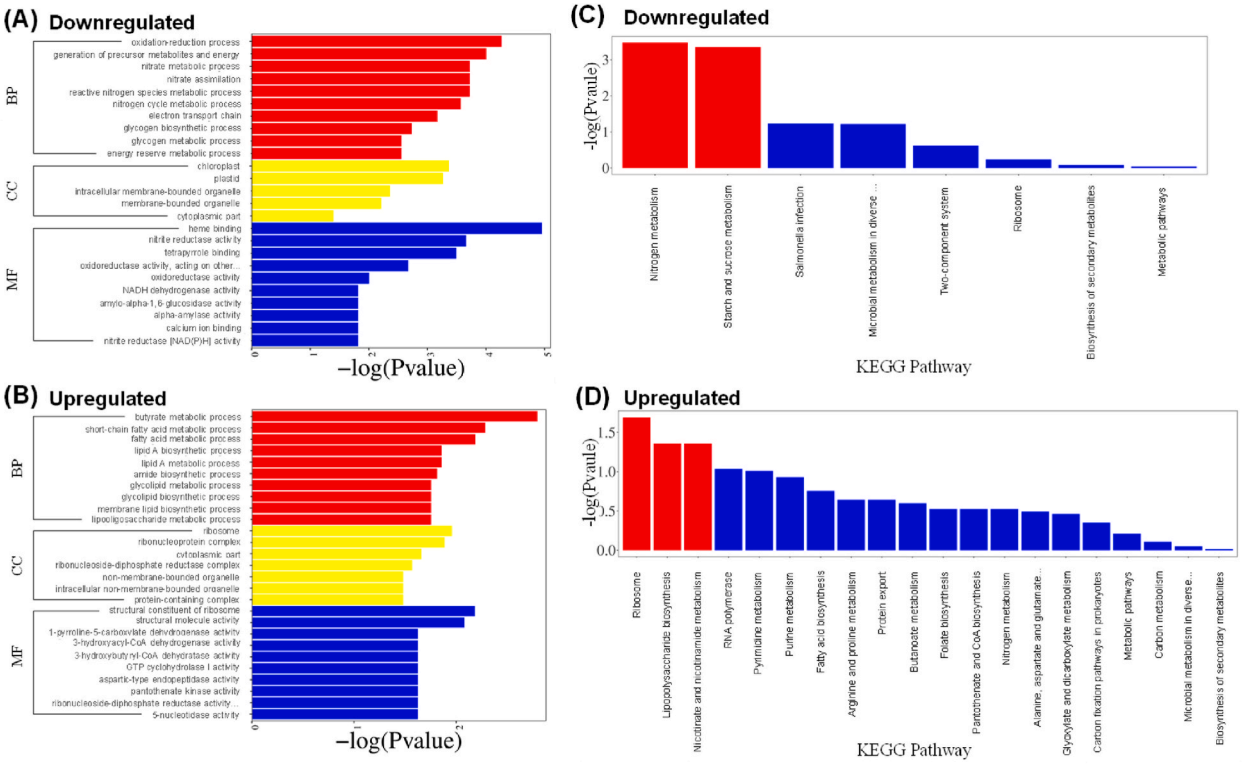

Fig. 6. Significant GO categories and KEGG pathways analysis for differentially expressed genes. For GO analysis, downregulated (A) and upregulated (B) genes in the test group vs. the control group. The ordinate axis is the GO category (Biological Process, BP; Cellular Component, CC; Molecular Function, MF), and the abscissa axis is the −log (*P* value) of GO categories. A maximum of 10 GOs are displayed per GO category. For KEGG analysis, downregulated (C) and upregulated (D) genes in the test group vs. the control group. The ordinate axis is the pathway category and the abscissa axis is the −log (*P* value) of the pathway category. Significant pathways (*P* value $\leq$ 0.05) are displayed in red, while nonsignificant pathways (*P* value > 0.05) are shown in blue.

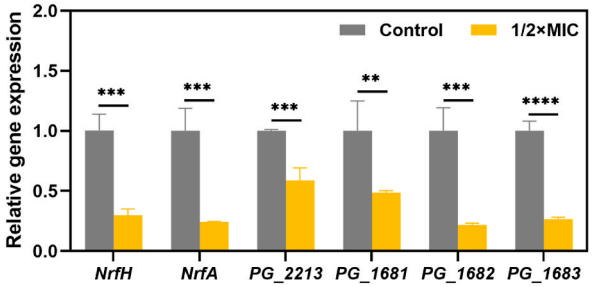

Fig. 7. Validation of selected genes in untreated *P. gingivalis* (control) and treated *P. gingivalis* with TC at 1/2 × MIC. Values are presented as mean ± SD with at least n = 3. Statistical significance was assessed using an unpaired two-tailed Student's t-test. ***P* < 0.01, ****P* < 0.001, and *****P* < 0.0001.

[51]. Arce et al. reported that oxidative stress in biofilms can affect their growth [52], and the observed biological process in the oxidation-reduction process was similar to our results regarding the effect of TC on *P. gingivalis* biofilms. Downregulated genes that correlated with molecular functions were primarily concentrated in haeme binding. Previous studies have shown that haeme binding plays a critical role in biofilm regulation [9]. Since *P. gingivalis* requires haeme for growth, survival, and virulence, it acquires haeme for efficient host colonisation during biofilm co-culture [53]. These findings may be another possible reason for TC restraining *P. gingivalis* biofilm.

KEGG pathway analysis demonstrated that the pathways influencing cell translation were enhanced, and the pathways controlling cell metabolism were mainly repressed, which was consistent with the results of the GO analysis. In this study, the ribosome pathway, which plays a vital role in cell translation, was the most significantly upregulated pathway. We found that five genes were upregulated in this pathway. For example, *Ribosomal Protein SA* (*RPSA*) is a membrane receptor of many pathogenic bacteria that induces the

adherence of pathogenic bacteria to host cells [54]. The upregulated expression of the ribosomal pathway verified again that it was not the antibacterial target of TC on *P. gingivalis*. In addition, the nitrogen metabolism and starch and sucrose metabolism pathways were significantly suppressed by TC treatment. *P. gingivalis* was reported to be a saccharolytic bacterium, which provides energy via nitrogen metabolism [55]. Downregulated nitrogen metabolism could inhibit the growth of *P. gingivalis*, and disruption of physiological metabolism might also impede *P. gingivalis* biofilm formation. Three genes were found to be downregulated in this pathway. *NrfA*, *NrfH*, and *PG_2213* encode cytochrome *c*-552, cytochrome *c* nitrite reductase subunit, and nitrite reductase-related proteins, respectively. *NrfH* acquires electrons from the menaquinone pool and mediates their transfer to the catalytic subunit *NrfA* in the anaerobic respiratory process of nitrite [56]. Starch and sucrose metabolism have profound effects not only on the polysaccharide matrix, but also on the dynamics of biofilm development and pathogenicity [57], partly explaining the anti-biofilm effect of TC. In this pathway, *PG_1681*, *PG_1682,* and *PG_1683* encode glycogen debranching enzyme, glycosyl transferase group 1 family protein, and glyco_hydro_57 domain-containing protein, respectively, which were downregulated and may be related to glycogen biosynthesis. Moreover, the differentially expressed genes in the downregulated signaling pathways were further confirmed by RT-qPCR. Therefore, this study concluded that TC inhibited the growth of *P. gingivalis* and biofilm formation, and altered the transcription of nitrogen metabolism and starch and sucrose metabolism-related genes.

There are still some limitations of this study. First, more than 700 bacterial species or phylotypes have been detected in the oral cavity [58]. Previous studies reported that both periodontitis and peri-implantitis have been linked with primarily Gram-negative anaerobes and polymicrobial infection, of which some core microbiota might play an important role [6,7]. This study only focused on one of the most frequently found pathogens associated with periodontitis and peri-implantitis—*P. gingivalis*. Further research is needed to verify the antibacterial effects of TC against other common periodontopathic bacteria, such as *Fusobacterium nucleatum*, *Aggregatibacter actinomycetemcomitans*, *Tannerella forsythia*, and so on, as well as polymicrobial biofilms. Second, this study preliminarily investigated the antibacterial activity of TC on *P. gingivalis* and examined its possible antibacterial mechanism in vitro. However, further studies are required to detect the antibacterial behavior of TC in vivo to reflect the conditions that occur clinically.

5. Conclusions

This study demonstrated the antimicrobial effect of TC on *P. gingivalis*, of which the MIC and MBC were 39.07 μg/mL and 78.13 μg/mL, respectively. After exposure to TC, 46 genes were downregulated in *P. gingivalis*. The pathways controlling cell metabolism were mainly repressed, among which the expression levels of selected genes correlated to nitrogen metabolism (*NrfA*, *NrfH* and *PG_2213*) and starch and sucrose metabolism (*PG_1681*, *PG_1682,* and *PG_1683*) showed significant inhibition. This finding confirmed TC to be a natural antimicrobial agent against *P. gingivalis* and further demonstrated that TC suppressed the microbial activity on *P. gingivalis* by disruption of physiological metabolism, which might inhibit the growth and the biofilm formation of *P. gingivalis*. This study provides further insight into the potential of TC to be used in adjunctive treatment of periodontitis and peri-implantitis.

Funding statement

This work was supported by the Fundamental Research Program Funding of Ninth People's Hospital affiliated to Shanghai Jiao Tong university School of Medicine [grant number JYZZ107]; the Cross-disciplinary Research Fund of Shanghai Ninth People's Hospital, Shanghai Jiao Tong university School of Medicine [grant number JYJC202202]; the Natural Science Foundation of Shanghai Municipal Science and Technology Commission [grant number 21ZR1437200, 23ZR1453600]. We would like to thank Editage (www.editage.cn) for English language editing.

Data availability statement

Data will be made available on request.

CRediT authorship contribution statement

Ning Gan: Writing – review & editing, Writing – original draft, Validation, Methodology, Formal analysis, Data curation, Conceptualization. **Yingjing Fang:** Writing – original draft, Validation, Methodology, Formal analysis, Data curation, Conceptualization. **Weimin Weng:** Software, Formal analysis. **Ting Jiao:** Writing – review & editing, Supervision, Resources, Project administration, Investigation, Funding acquisition. **Weiqiang Yu:** Writing – review & editing, Supervision, Resources, Project administration, Methodology, Investigation, Funding acquisition.

Declaration of competing interest

The authors declare that they have no known competing financial interests or personal relationships that could have appeared to influence the work reported in this paper.

Appendix A. Supplementary data

Supplementary data to this article can be found online at https://doi.org/10.1016/j.heliyon.2023.e23048.

References

[1] D. Richards, Review finds that severe periodontitis affects 11% of the world population, Evid. Base Dent. 15 (2014) 70–71.
[2] O.M. Goudouri, E. Kontonasaki, U. Lohbauer, A.R. Boccaccini, Antibacterial properties of metal and metalloid ions in chronic periodontitis and peri-implantitis therapy, Acta Biomater. 10 (2014) 3795–3810.
[3] M.S. Tonetti, S. Jepsen, L. Jin, J. Otomo-Corgel, Impact of the global burden of periodontal diseases on health, nutrition and wellbeing of mankind: a call for global action, J. Clin. Periodontol. 44 (2017) 456–462.
[4] R. Tzach-Nahman, G. Mizraji, L. Shapira, G. Nussbaum, A. Wilensky, Oral infection with Porphyromonas gingivalis induces peri-implantitis in a murine model: evaluation of bone loss and the local inflammatory response, J. Clin. Periodontol. 44 (2017) 739–748.
[5] M. Aljateeli, J.H. Fu, H.L. Wang, Managing peri-implant bone loss: current understanding, Clin. Implant Dent. Relat. Res. 14 (Suppl 1) (2012) e109–e118.
[6] G.I. Lafaurie, M.A. Sabogal, D.M. Castillo, M.V. Rincon, L.A. Gomez, Y.A. Lesmes, L. Chambrone, Microbiome and microbial biofilm profiles of peri-implantitis: a systematic review, J. Periodontol. 88 (2017) 1066–1089.
[7] A. Kensara, E. Hefni, M.A. Williams, H. Saito, E. Mongodin, R. Masri, Microbiological profile and human immune response associated with peri-implantitis: a systematic review, J. Prosthodont. 30 (2020) 210–234.
[8] S.C. Holt, J. Ebersole, J. Felton, M. Brunsvold, K.S. Kornman, Implantation of Bacteroides gingivalis in nonhuman primates initiates progression of periodontitis, Science 239 (1988) 55–57.
[9] J. Fu, S. Hall, E.M. Boon, Recent evidence for multifactorial biofilm regulation by heme sensor proteins NosP and H-NOX, Chem. Lett. 50 (2021) 1095–1103.
[10] A. Al-Ahmad, F. Muzafferiy, A.C. Anderson, J.P. Wolber, P. Ratka-Kruger, T. Fretwurst, K. Nelson, K. Vach, E. Hellwig, Shift of microbial composition of peri-implantitis-associated oral biofilm as revealed by 16S rRNA gene cloning, J. Med. Microbiol. 67 (2018) 332–340.
[11] J. Azelmat, J.F. Larente, D. Grenier, The anthraquinone rhein exhibits synergistic antibacterial activity in association with metronidazole or natural compounds and attenuates virulence gene expression in Porphyromonas gingivalis, Arch. Oral Biol. 60 (2015) 342–346.
[12] E. Varon-Shahar, A. Shusterman, A. Piattelli, G. Iezzi, E.I. Weiss, Y. Houri-Haddad, Peri-implant alveolar bone resorption in an innovative peri-implantitis murine model: effect of implant surface and onset of infection, Clin. Implant Dent. Relat. Res. 21 (2019) 723–733.
[13] M. Saita, J. Kaneko, T. Sato, S.S. Takahashi, S. Wada-Takahashi, R. Kawamata, T. Sakurai, M.C. Lee, N. Hamada, K. Kimoto, Y. Nagasaki, Novel antioxidative nanotherapeutics in a rat periodontitis model: reactive oxygen species scavenging by redox injectable gel suppresses alveolar bone resorption, Biomaterials 76 (2016) 292–301.
[14] E. Blank, J. Grischke, A. Winkel, J. Eberhard, N. Kommerein, K. Doll, I. Yang, M. Stiesch, Evaluation of biofilm colonization on multi-part dental implants in a rat model, BMC Oral Health 21 (2021) 313.
[15] C. Zenobia, G. Hajishengallis, Porphyromonas gingivalis virulence factors involved in subversion of leukocytes and microbial dysbiosis, Virulence 6 (2015) 236–243.
[16] G. Hajishengallis, R.P. Darveau, M.A. Curtis, The keystone-pathogen hypothesis, Nat. Rev. Microbiol. 10 (2012) 717–725.
[17] Y. Wang, Y. Zhang, Y.Q. Shi, X.H. Pan, Y.H. Lu, P. Cao, Antibacterial effects of cinnamon (Cinnamomum zeylanicum) bark essential oil on Porphyromonas gingivalis, Microb. Pathog. 116 (2018) 26–32.
[18] A. Ahmad, A.M. Viljoen, H.Y. Chenia, The impact of plant volatiles on bacterial quorum sensing, Lett. Appl. Microbiol. 60 (2015) 8–19.
[19] J. Kolozsváriné Nagy, Á.M. Móricz, A. Böszörményi, Á. Ambrus, I. Schwarczinger, Antibacterial effect of essential oils and their components against Xanthomonas arboricola pv. pruni revealed by microdilution and direct bioautographic assays, Front. Cell. Infect. Microbiol. 13 (2023), 1204027.
[20] Y. Ou, M. Yan, G. Gao, W. Wang, Q. Lu, J. Chen, Cinnamaldehyde protects against ligature-induced periodontitis through the inhibition of microbial accumulation and inflammatory responses of host immune cells, Food Funct. 13 (2022) 8091–8106.
[21] X. Yan, A.A. Wardana, L.P. Wigati, F. Meng, S. Leonard, F.N. Nkede, F. Tanaka, F. Tanaka, Characterization and bio-functional performance of chitosan/poly (vinyl alcohol)/trans-cinnamaldehyde ternary biopolymeric films, Int. J. Biol. Macromol. 246 (2023), 125680.
[22] E.G. Gulec PekerK. Kaltalioglu, Cinnamaldehyde and eugenol protect against LPS-stimulated oxidative stress and inflammation in Raw 264.7 cells, J. Food Biochem. 45 (2021), e13980.
[23] C. Park, H. Lee, S. Hong, I.M.N. Molagoda, J.W. Jeong, C.Y. Jin, G.Y. Kim, S.H. Choi, S.H. Hong, Y.H. Choi, Inhibition of lipopolysaccharide-induced inflammatory and oxidative responses by trans-cinnamaldehyde in C2C12 myoblasts, Int. J. Med. Sci. 18 (2021) 2480–2492.
[24] A.M. Omar, M.E. El-Araby, T.M. Abdelghany, M.K. Safo, M.H. Ahmed, R. Boothello, B.B. Patel, M.S. Abdel-Bakky, A.M. Malebari, H.E.A. Ahmed, R.S. Elhaggar, Introducing of potent cytotoxic novel 2-(aroylamino)cinnamamide derivatives against colon cancer mediated by dual apoptotic signal activation and oxidative stress, Bioorg. Chem. 101 (2020), 103953.
[25] Y.F. Chiang, H.Y. Chen, K.C. Huang, P.H. Lin, S.M. Hsia, Dietary antioxidant trans-cinnamaldehyde reduced visfatin-induced breast cancer progression: in vivo and in vitro study, Antioxidants 8 (2019) 625.
[26] G.R. Gandhi, V.E. Hillary, P.J. Antony, L.L.D. Zhong, D. Yogesh, N.M. Krishnakumar, S.A. Ceasar, R.Y. Gan, A systematic review on anti-diabetic plant essential oil compounds: dietary sources, effects, molecular mechanisms, and safety, Crit. Rev. Food Sci. Nutr. (2023) 1–20.
[27] H. Zhao, H. Wu, M. Duan, R. Liu, Q. Zhu, K. Zhang, L. Wang, Cinnamaldehyde improves metabolic functions in streptozotocin-induced diabetic mice by regulating gut microbiota, Drug Des. Dev. Ther. 15 (2021) 2339–2355.
[28] D.A. Elsherbiny, A.M. Abdelgawad, B.A. Hemdan, A.S. Montaser, I.E. El-Sayed, S. Jockenhoevel, S. Ghazanfari, Self-crosslinked polyvinyl alcohol/cellulose nanofibril cryogels loaded with synthesized aminophosphonates as antimicrobial wound dressings, J. Mater. Chem. B 11 (2023) 7144–7159.
[29] M. Ribeiro, J. Malheiro, L. Grenho, M.H. Fernandes, M. Simoes, Cytotoxicity and antimicrobial action of selected phytochemicals against planktonic and sessile Streptococcus mutans, PeerJ 6 (2018), e4872.
[30] Z. He, Z. Huang, W. Jiang, W. Zhou, Antimicrobial activity of cinnamaldehyde on Streptococcus mutans biofilms, Front. Microbiol. 10 (2019) 2241.
[31] M. Hu, S. Kalimuthu, C. Zhang, I.A.A. Ali, P. Neelakantan, Trans-cinnamaldehyde-Biosurfactant complex as a potent agent against Enterococcus faecalis biofilms, Pharmaceutics 14 (2022) 2355.
[32] J.O.E. Nogueira, G.A. Campolina, L.R. Batista, E. Alves, A.R.S. Caetano, R.M. Brandao, D.L. Nelson, M.D.G. Cardoso, Mechanism of action of various terpenes and phenylpropanoids against Escherichia coli and Staphylococcus aureus, FEMS Microbiol. Lett. 368 (2021) fnab052.
[33] N. Ullah, A. Amin, A. Farid, S. Selim, S.A. Rashid, M.I. Aziz, S.H. Kamran, M.A. Khan, N. Rahim Khan, S. Mashal, M. Mohtasheemul Hasan, Development and evaluation of essential oil-based nanoemulgel formulation for the treatment of oral bacterial infections, Gels 9 (2023), 252.
[34] N. Gan, W. Qin, C. Zhang, T. Jiao, One-step in situ deposition of phytic acid-metal coordination complexes for combined Porphyromonas gingivalis infection prevention and osteogenic induction, J. Mater. Chem. B (2022) 4293–4305.
[35] M. Ashburner, C.A. Ball, J.A. Blake, D. Botstein, H. Butler, J.M. Cherry, A.P. Davis, K. Dolinski, S.S. Dwight, J.T. Eppig, M.A. Harris, D.P. Hill, L. Issel-Tarver, A. Kasarskis, S. Lewis, J.C. Matese, J.E. Richardson, M. Ringwald, G.M. Rubin, G. Sherlock, Gene ontology: tool for the unification of biology. The Gene Ontology Consortium, Nat. Genet. 25 (2000) 25–29.
[36] M. Kanehisa, The KEGG database, Novartis Found. Symp. 247 (2002) 91–101, discussion 101-103, 119-128, 244-252.
[37] W.L. Du, S.S. Niu, Y.L. Xu, Z.R. Xu, C.L. Fan, Antibacterial activity of chitosan tripolyphosphate nanoparticles loaded with various metal ions, Carbohydr. Polym. 75 (2009) 385–389.
[38] J. Gong, L. Yang, Q. He, T. Jiao, In vitro evaluation of the biological compatibility and antibacterial activity of a bone substitute material consisting of silver-doped hydroxyapatite and Bio-Oss((R)), J. Biomed. Mater. Res., Part B 106 (2018) 410–420.
[39] M.C. Duarte, E.E. Leme, C. Delarmelina, A.A. Soares, G.M. Figueira, A. Sartoratto, Activity of essential oils from Brazilian medicinal plants on Escherichia coli, J. Ethnopharmacol. 111 (2007) 197–201.
[40] S.A. Saquib, N.A. AlQahtani, I. Ahmad, M.A. Kader, S.S. Al Shahrani, E.A. Asiri, Evaluation and comparison of antibacterial efficacy of herbal extracts in combination with antibiotics on periodontal pathobionts: an in vitro microbiological study, Antibiotics (Basel) 8 (2019) 89.

[41] H. Chouirfa, H. Bouloussa, V. Migonney, C. Falentin-Daudre, Review of titanium surface modification techniques and coatings for antibacterial applications, Acta Biomater. 83 (2019) 37–54.
[42] J. Grischke, J. Eberhard, M. Stiesch, Antimicrobial dental implant functionalization strategies -A systematic review, Dent. Mater. J. 35 (2016) 545–558.
[43] E. Szentirmai, N.S. Millican, A.R. Massie, L. Kapas, Butyrate, a metabolite of intestinal bacteria, enhances sleep, Sci. Rep. 9 (2019) 7035.
[44] S.C. Bridgeman, W. Northrop, P.E. Melton, G.C. Ellison, P. Newsholme, C.D.S. Mamotte, Butyrate generated by gut microbiota and its therapeutic role in metabolic syndrome, Pharmacol. Res. 160 (2020), 105174.
[45] P. Amiri, S.A. Hosseini, S. Ghaffari, H. Tutunchi, S. Ghaffari, E. Mosharkesh, S. Asghari, N. Roshanravan, Role of butyrate, a gut microbiota derived metabolite, in cardiovascular diseases: a comprehensive narrative review, Front. Pharmacol. 12 (2021), 837509.
[46] K.M. Byrd, A.S. Gulati, The "Gum-Gut" Axis in inflammatory bowel diseases: a hypothesis-driven review of associations and advances, Front. Immunol. 12 (2021), 620124.
[47] J. Chung, S. Kim, H.A. Lee, M.H. Park, S. Kim, Y.R. Song, H.S. Na, Trans-cinnamic aldehyde inhibits Aggregatibacter actinomycetemcomitans-induced inflammation in THP-1-derived macrophages via autophagy activation, J. Periodontol. 89 (2018) 1262–1271.
[48] S.L. Qu, L. Chen, X.S. Wen, J.P. Zuo, X.Y. Wang, Z.J. Lu, Y.F. Yang, Suppression of Th17 cell differentiation via sphingosine-1-phosphate receptor 2 by cinnamaldehyde can ameliorate ulcerative colitis, Biomed, Pharmacother 134 (2021), 111116.
[49] D.N. Wilson, Ribosome-targeting antibiotics and mechanisms of bacterial resistance, Nat. Rev. Microbiol. 12 (2014) 35–48.
[50] Y. Kim, J. Jeon, M.S. Kwak, G.H. Kim, I. Koh, M. Rho, Photosynthetic functions of Synechococcus in the ocean microbiomes of diverse salinity and seasons, PLoS One 13 (2018), e0190266.
[51] D.J. Betteridge, What is oxidative stress? Metabolism 49 (2000) 3–8.
[52] J.E. Arce Miranda, C.E. Sotomayor, I. Albesa, M.G. Paraje, Oxidative and nitrosative stress in Staphylococcus aureus biofilm, FEMS Microbiol. Lett. 315 (2011) 23–29.
[53] P. Slezak, M. Smiga, J.W. Smalley, K. Sieminska, T. Olczak, Porphyromonas gingivalis HmuY and Streptococcus gordonii GAPDH-novel heme acquisition strategy in the oral microbiome, Int. J. Mol. Sci. 21 (2020) 4150.
[54] C.J. Orihuela, J. Mahdavi, J. Thornton, B. Mann, K.G. Wooldridge, N. Abouseada, N.J. Oldfield, T. Self, D.A. Ala'Aldeen, E.I. Tuomanen, Laminin receptor initiates bacterial contact with the blood brain barrier in experimental meningitis models, J. Clin. Invest. 119 (2009) 1638–1646.
[55] D. Grenier, P. Gauthier, P. Plamondon, K. Nakayama, D. Mayrand, Studies on the aminopeptidase activities of Porphyromonas gingivalis, Oral Microbiol. Immunol. 16 (2001) 212–217.
[56] M.L. Rodrigues, T.F. Oliveira, I.A. Pereira, M. Archer, X-ray structure of the membrane-bound cytochrome c quinol dehydrogenase NrfH reveals novel haem coordination, EMBO J. 25 (2006) 5951–5960.
[57] M.I. Klein, L. DeBaz, S. Agidi, H. Lee, G. Xie, A.H. Lin, B.R. Hamaker, J.A. Lemos, H. Koo, Dynamics of Streptococcus mutans transcriptome in response to starch and sucrose during biofilm development, PLoS One 5 (2010), e13478.
[58] J.A. Aas, B.J. Paster, L.N. Stokes, I. Olsen, F.E. Dewhirst, Defining the normal bacterial flora of the oral cavity, J. Clin. Microbiol. 43 (2005) 5721–5732.